3rd EUROPEAN CONFERENCE ON
EARTHQUAKE ENGINEERING & SEISMOLOGY
BUCHAREST, ROMANIA, 2022

Condensed-tangent-stiffness-proportional viscous damping model for nonlinear time history analysis

Jose Fernando Baena-Urrea – PhD student, Institute of Mechanics, Materials and Civil Engineering, UCLouvain, Belgium, jose.baenaurrea@uclouvain.be

João Pacheco de Almeida – Assistant Professor, Institute of Mechanics, Materials and Civil Engineering, UCLouvain, Belgium, joao.almeida@uclouvain.be

Abstract: This work explains the development of a viscous damping model using the condensed tangent stiffness of the structure. It eliminates the spurious damping forces and avoids the high levels of damping presented by the condensed damping model defined with the initial properties. Additionally, this article elucidates some of the problems of the existing condensed models and compares them with Rayleigh or total initial stiffness proportional damping. The proposed damping model and the existing models are compared using a reinforced concrete frame subjected to a ground motion, where the main arguments to justify the newly proposed damping model are highlighted.

Keywords: time-history analysis, viscous damping, condensed damping models.

1. Introduction

Nonlinear analyses are commonly used in research and specialized structural engineering practice due to the community's growing interest in performance-based design, the use of seismic control systems, and the assessment of existing structures (Golesorkhi et al. 2017). The system of equations expressing dynamic equilibrium for a viscous damped nonlinear multi-degree-of-freedom (MDoF) planar system subjected to earthquake and gravity (or static) loading is given in the next equation. It is noted that a viscous damping model is employed, which is commonly the case, which models the energy dissipation mechanisms that are independent of the material hysteretic rules (Chrisp 1980; Bernal 1994).

$$\begin{bmatrix} \boldsymbol{M}_{tt} & 0 \\ 0 & 0 \end{bmatrix} \begin{Bmatrix} \ddot{\boldsymbol{U}}_t(t) \\ \ddot{\boldsymbol{U}}_0(t) \end{Bmatrix} + \begin{bmatrix} \boldsymbol{C}_{tt} & \boldsymbol{C}_{t0} \\ \boldsymbol{C}_{0t} & \boldsymbol{C}_{00} \end{bmatrix} \begin{Bmatrix} \dot{\boldsymbol{U}}_t(t) \\ \dot{\boldsymbol{U}}_0(t) \end{Bmatrix} + \{\boldsymbol{f}(\boldsymbol{U}(t))\} = \begin{Bmatrix} -\boldsymbol{M}_{tt}\boldsymbol{J}_x \ddot{u}_{gx}(t) \\ 0 \end{Bmatrix} + \begin{Bmatrix} \boldsymbol{P}_{gt} \\ \boldsymbol{P}_{g0} \end{Bmatrix} \tag{1}$$

where $\boldsymbol{M}$ and $\boldsymbol{C}$ are the mass and damping matrices, respectively, and $\{\boldsymbol{f}(\boldsymbol{U}(t))\}$ represents the nonlinear relation between resisting forces and displacements. The subscripts *t* and *0* refer to the degrees of freedoms (DoFs) with and without mass, which is an essential separation for inertial loadings. The vectors $\boldsymbol{U}$, $\dot{\boldsymbol{U}}$, and $\ddot{\boldsymbol{U}}$ are the vectors of relative displacement, velocity, and acceleration of the DoFs. The right side of the equation contains two loading vectors corresponding to a time-varying component and a constant term. The former represents the effective earthquake forces in the *x*-direction, where $\boldsymbol{J}_x$ is the influence vector and $\ddot{u}_{gx}(t)$ is the corresponding component of the ground motion acceleration record. The gravity or static forces $\begin{Bmatrix} \boldsymbol{P}_{gt} \\ \boldsymbol{P}_{g0} \end{Bmatrix}$ can be applied in all the DoFs of the structure.

The damping matrix $\boldsymbol{C}$ is often defined with the viscous damping model proposed by Lord Rayleigh (Rayleigh 1877). This model is defined by equation (2) using the mass matrix and, originally, the initial stiffness matrix as proportionality matrices. The latter are multiplied by two damping parameters found with equation (3) based on two selected frequencies (ω_i, ω_j) and a damping ratio ascribed to each frequency (ζ_i, ζ_j).

$$\begin{bmatrix} \boldsymbol{C}_{tt} & \boldsymbol{C}_{t0} \\ \boldsymbol{C}_{0t} & \boldsymbol{C}_{00} \end{bmatrix} = a_0 \begin{bmatrix} \boldsymbol{M}_{tt} & 0 \\ 0 & 0 \end{bmatrix} + a_1 \begin{bmatrix} \boldsymbol{K}_{tt} & \boldsymbol{K}_{t0} \\ \boldsymbol{K}_{0t} & \boldsymbol{K}_{00} \end{bmatrix} \tag{2}$$

$$\begin{Bmatrix} \zeta_i \\ \zeta_j \end{Bmatrix} = \frac{1}{2} \begin{bmatrix} \omega_i^{-1} & \omega_i \\ \omega_j^{-1} & \omega_j \end{bmatrix} \begin{Bmatrix} a_0 \\ a_1 \end{Bmatrix} \tag{3}$$

Since the assigned damping ratios are small for common civil engineering structures analysed as linear elastic systems, the damping forces are also limited and consequently the inconsistencies of Rayleigh damping (RD) do not significantly affect the structural response. For instance, in a linear single-degree-of-freedom (SDoF) where a damping ratio of 5% is defined, the damping force may reach approximately 10% of the inertial or elastic forces of the structure (Carr 2007). With this argument, Wilson and Clough (1962) mentioned that it was justifiable to use this model for step-by-step linear dynamic analyses of MDoF systems, recognizing that the exact form of damping in most structures is unknown.

The above rationale for using this model in nonlinear analyses is no longer valid. The damping forces for an inelastic SDoF defined with 5% of critical damping may reach 20% of the inertial or material resisting forces (Carr 2007). During incursions in the inelastic range, the stiffness proportional term of RD triggers significant damping moments in the rotational massless DoFs reaching important magnitudes (Bernal 1994) and leads to an overall change in the effective damping ratio of the system during the analysis (Charney 2008), which has no physical justification and leads to unconservative analyses (Medina and Krawinkler 2003). For instance, underestimation of peak displacement demands, overestimation of peak strength demands. Despite the advantages of the mass proportional term (Correia et al. 2013), it has also been criticized because it can lead to high damping forces (Erduran 2012). In base isolated systems, Ryan and Polanco (2008) mentioned that the mass-proportional component of RD can generate unconservative analyses.

Almost since the implementation of RD in nonlinear dynamic analysis, commercial and research FE software also allowed to define the damping matrix proportional to the tangent stiffness matrix (Kanaan and Powell 1973; Powell 1973; Sharpe 1974; Mondkar and Powell 1975). Recent studies, e.g. by Petrini et al. (2008), Jehel et al. (2014), and Chambreuil et al. (2021), recommend the use of this method because spurious damping forces are significantly reduced and overall better match with experimental results. Leger and Dussault (1992) and Charney (2008) proposed to update the coefficients a_o and a_1, at each step of the analysis, using the tangent stiffness matrix to find the frequencies of the structure and recalculate the coefficients using eq. (3). According to those authors, this methodology preserves a constant damping ratio throughout the analysis and artificial damping is eliminated. However, updating the damping parameters has in general an important computational cost.

Specific issues arising by the use of a tangent damping matrix were described early in ANSI-I (Mondkar and Powell 1975) and DRAIN2D (Kanaan and Powell 1973). They include low damping forces when the structure yields and possible equilibrium unbalances that need to be accounted for, caused by the fact that the stiffness matrix of the previously converged step is normally used to define the damping matrix for the next step. More recently, Chopra and Mckenna (2016) argued that the model has several conceptual limitations, including damping force-velocity relations exhibiting hysteresis due to the reformulation of the damping matrix at each step, and negative damping at large deformations. The former issue may be avoided as discussed by Correia et al. (2013). Other investigations (Bernal 1994; Carr 2007; Chopra and Mckenna 2016) have proposed to define non-null entries of the viscous damping matrix just for the entries connecting two DOFs with mass, the so-called condensed damping models, which implies that the damping forces and moments are completely eliminated in the massless DoF.

The present paper aims at proposing a damping model proportional to the condensed stiffness matrix – in opposition to the total stiffness matrix – using the tangent stiffness matrix, which has not yet been explored in the literature. The motivation is introduced in the next section. The paper compares the behaviour of existing total and condensed damping models using a reinforced concrete (RC) frame subjected to a ground-motion loading, where numerical deficiencies of existing condensed damping models are highlighted. These numerical deficiencies are the main arguments justifying the proposed damping model, which is introduced following a review of existing condensed damping models. Section 3 compares a set of existing damping models for the study case referred above. Finally, the last section sums up the main conclusions.

2. Condensed-tangent-stiffness-proportional damping model

2.1. Motivation

Condensed damping models are those defined only in the degrees of freedom with mass and include: mass proportional damping (MPD), condensed initial-stiffness proportional damping (CISPD) as proposed by Bernal (1994), and the modal damping (MD) proposed by Wilson and Penzien (1972) for elastic response and later implemented for inelastic analyses by Carr (2007) and Chopra and Mckenna (2016). The main advantages of condensed damping models are the complete elimination of spurious damping forces and the fact that the damping matrix must be calculated only in one step of the analysis, which is preferable from a computational cost point of view.

Even if spurious damping forces are eliminated with condensed models, they can cause an overdamped response in the structure due to the stiffness decay, implying levels of energy dissipation similar to the total initial stiffness proportional damping model (TISPD) or RD with ISPD, which are generally considered as inappropriate by the engineering community, see section 3. Additionally, except for MPD, all the other condensed damping models imply the occurrence of dashpots between the DoFs that are not physically connected by a structural element, which is regularly criticized (Hall 2016; Charney et al. 2017). Finally, Lanzi and Luco (2018) highlighted that the massless DoFs present significant oscillations on their velocity when step-by-step integration procedures are used, e.g. for nonlinear dynamic analysis of real structures. The mentioned issues are the motivation to study these models further and explore a new proposal.

2.2. Existing condensed damping models

2.2.1. Mass proportional damping model

The mass-proportional damping model is a particular case of the RD model presented in eq. (2) where just the first term is considered; the damping parameter is found as:

$$a_0 = 2\zeta_i\omega_i \tag{4}$$

2.2.2. Condensed initial stiffness proportional damping model

Bernal (1994) proposed a condensed-initial-stiffness-proportional (CISPD) damping model to eliminate the spurious damping forces in the massless DoFs. The author recognized that an MPD model also solves this pathology. However, the study mentioned that condensed stiffness preserves the potential to use the stiffness matrix without being affected by spurious damping forces. This model can be expressed as:

$$\begin{bmatrix} \boldsymbol{C}_{tt} & \boldsymbol{C}_{t0} \\ \boldsymbol{C}_{0t} & \boldsymbol{C}_{00} \end{bmatrix} = \begin{bmatrix} \boldsymbol{C}_{tt} & 0 \\ 0 & 0 \end{bmatrix} = a_1 \begin{bmatrix} \widehat{\boldsymbol{K}}_{tt} & 0 \\ 0 & 0 \end{bmatrix} \tag{5}$$

where $\widehat{\boldsymbol{K}}_{tt}$ is the condensed stiffness matrix given by the next equation in terms of submatrices of the total initial stiffness matrix.

$$\widehat{\boldsymbol{K}}_{tt} = \boldsymbol{K}_{tt} - \boldsymbol{K}_{0t}^{t} \boldsymbol{K}_{00}^{-1} \boldsymbol{K}_{0t} \tag{6}$$

2.2.3. Caughey damping model

Caughey damping model is a generalization of Rayleigh damping where is possible to assign *N* distinct damping ratios. This model is expressed by eq. (7):

$$\boldsymbol{C} = \boldsymbol{M} \sum_{i=0}^{N-1} a_i [\boldsymbol{M}^{-1} \boldsymbol{K}]^i \tag{7}$$

where the damping parameters a_i are defined solving the next system of equations:

$$\zeta_n = \frac{1}{2} \sum_{i=0}^{N-1} a_i \omega_n^{2i-1} \tag{8}$$

Caughey damping presents some numerical difficulties explained by (Chopra (2015) for linear analysis. For example, the expression (8) used to find the damping parameters is often numerically ill-conditioned due to the difference between the order of magnitude of the frequencies. Additionally, when more than two terms are considered in equation (7), the damping matrix becomes fully populated in systems without massless DOFs.

In common systems with massless DOFs, the total mass and stiffness matrix cannot be used because the total mass matrix does not have inverse. Thus, the model must be defined using the mass matrix ($\boldsymbol{M}_{tt}$) and the initial condensed stiffness matrix ($\widehat{\boldsymbol{K}}_{tt}$), according to Eq. (9).

$$\boldsymbol{C} = \boldsymbol{M}_{tt} \sum_{i=0}^{N-1} a_i \left[\boldsymbol{M}_{tt}^{-1} \widehat{\boldsymbol{K}}_{tt}\right]^i \tag{9}$$

2.2.4. Modal damping (MD)

Wilson and Penzien (1972) proposed a direct and efficient procedure to define a damping matrix that overcomes the difficulties of the Caughey series for linear analysis. Similarly to Caughey damping, this model allows to define a specific damping ratio for more than two frequencies, eliminating the important levels of damping in higher modes of vibration that RD imposes. Recently, Chopra and Mckenna (2016) proposed to use this model in nonlinear dynamic analysis and demonstrated that the definition of damping for all the modes is not required to get an accurate response of the system. The study did not propose a criterion on how many modal frequencies should be considered.

$$\boldsymbol{C} = \boldsymbol{M}_{tt}\left(\sum_{n=1}^{N}\left(\frac{2\zeta_n\omega_n}{\boldsymbol{M}_g}\right)\boldsymbol{\Phi}_n\boldsymbol{\Phi}_n^t\right)\boldsymbol{M}_{tt} \tag{10}$$

2.3. Formulation and implementation of a condensed-tangent-stiffness damping

As discussed above, Bernal (1994) proposed a damping model proportional to the condensed initial stiffness matrix to eliminate spurious damping forces. This model imposes zero damping between the massless degrees of freedom, which solves the problem of high damping forces or moments in these DoFs during incursions in the inelastic range. However, as shown in the next section, this model and MD can depict high levels of energy dissipation. The following section shows that the energy dissipation in these models is very similar to TISPD or RD (defined with the initial stiffness matrix), which are usually considered inappropriate for nonlinear dynamic analysis.

Until now, from the extensive literature review, the damping model that appears to better fit experimental test results, on average, is the total tangent stiffness proportional damping model, which however does not eliminate spurious damping moments. The model explored in the present investigation seeks to combine the above desirable feature of tangent-stiffness proportionality with the main advantage of condensed models, i.e. the elimination of spurious damping moments. Therefore, the proposed model can be expressed by the following expression:

$$\boldsymbol{C}^{Tan} = a_{0,initial}\cdot\begin{bmatrix}\boldsymbol{M}_{tt} & 0\\ 0 & 0\end{bmatrix} + a_{1,initial}\begin{bmatrix}\widehat{\boldsymbol{K}}_{tt}^{Tan} & 0\\ 0 & 0\end{bmatrix} \tag{11}$$

where $\widehat{\mathbf{K}}_{\mathrm{tt}}^{\mathrm{Tan}}$ is the condensed tangent stiffness matrix found with eq. (6).

3. Numerical case study

Figure 1 presents the structure used to compare a series of different viscous damping models. The RC structure is modelled using force-based elements, which consider distributed plasticity using four integration points (Calabrese et al. 2010). For simplicity, cross-section "Section 1" is used for all the columns, while cross-section "Section 2" is assigned to all the beams. The material rules considered are shown in Table 1. The model by Menegotto and Pinto (1973) was used to simulate the behaviour of all the steel fibres. The concrete fibres were simulated using the model by Mander et al. (1988), but with different input parameters to consider the different degrees of confinement. The tensile strength of the concrete was neglected.

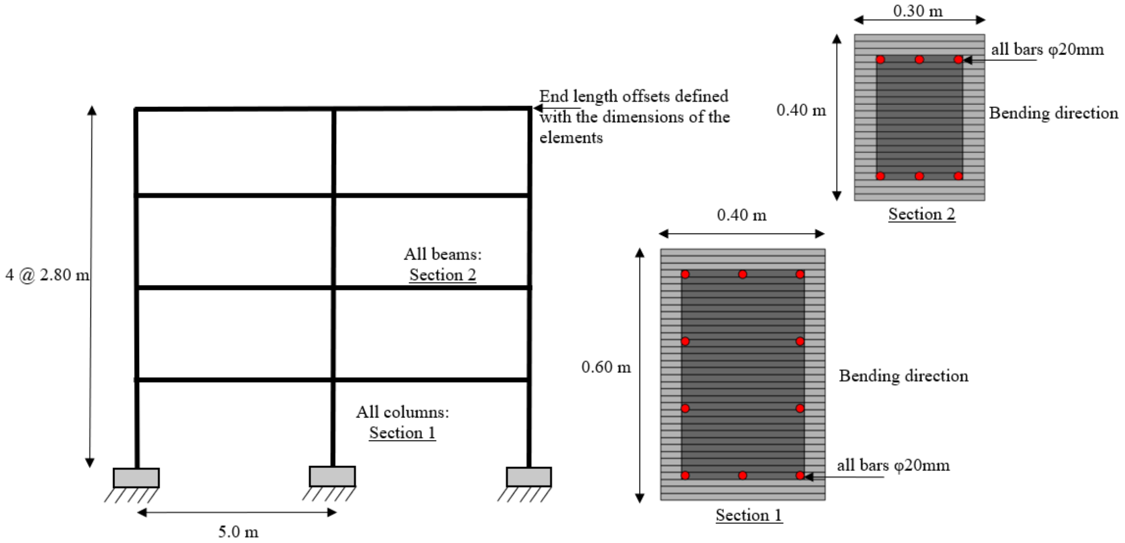

Fig. 1 - RC frame using distributed plasticity elements with section discretization on the right.

A corotational formulation was employed to account for the nonlinear geometric effects, and rigid length offsets at the nodes were defined according to the dimensions of the structural members. All the masses are lumped at the nodes in the horizontal and vertical directions. Masses of 8.92 ton and 17.86 ton are considered at the central and edge nodes, respectively. One horizontal acceleration ground motion record of the Morgan Hills earthquake is applied to the structure. The dynamic analysis is performed with the authors' software (SAGRES) using the Newmark integration method ($\beta = 1/4$ and $\gamma = ½$) and a Newton-Raphson scheme.

Table 1 Parameters of the material models assigned to the section fibres

Steel Fibres	**f_y (MPa)**	**E_o (GPa)**	**b**	**R0**	**A_1**	**A_2**	**A_3**	**A_4**
Steel bars	515	210	0.00	20.00	19.25	0.15	0.00	1.00
Concrete Fibres	**f_c (MPa)**	**E_o (GPa)**	**ε_{cu}**	**f_t (MPa)**	**ε_t**	**beta**		
Concrete cover	39.0	29.4	0.004	0	0	0.1		
Column's concrete core	52.7	39.6	0.018	0	0	0.1		
Beam's concrete core	46.0	34.6	0.014	0	0	0.1		

The damping models are described in Table 2, which includes a classification according to the positions in which the damping matrix is non-null: all DoFs or only DoFs with mass. The damping parameters are calculated using the initial frequencies of the structure and modal damping uses the initial modal shapes. All damping models are defined with a damping ratio of 3%.

Table 2 Damping models presented

Complete name	Nomenclature	Non-null values in the damping matrix defined at:
Total initial stiffness proportional damping	TISPD	all DoFs
Condensed initial stiffness proportional damping	CISPD	DoFs with mass
Total initial Rayleigh damping	RD	all DoFs
Modal damping (all modes included)	MD	DoFs with mass
Total tangent stiffness proportional damping	TTSPD	all DoFs
Condensed tangent stiffness proportional damping	CTSPD	DoFs with mass

The analysis of the structural response starts with the energy balance analysis presented in Fig. 2, where the total energy input (E_I), the cumulative energy dissipated by the damping model (E_D), and the energy dissipated by the material hysteretic rules (E_M) are shown.

Fig. 2(a) shows that the input energy is higher in those models proportional to the initial stiffness matrix (i.e., TISPD, CISPD, MD, and RD), while the damping models based on the tangent stiffness matrix present smaller energy input levels (i.e., TTSPD and CTSPD). The E_I is dissipated by the damping model or by the hysteretic rules of the material. The latter can be used to determine the structural performance and the damage on the structural elements through damage index models.

The damping models that dissipate more energy are those based on the initial properties of the system (TISPD, CISPD, MD, and RD, in descending order) and those that dissipate less energy are those proportional to the tangent stiffness matrix (TTSPD and CTSPD). Fig. 2(b) indicates that the energy dissipated by TISPD and CISPD are very similar, which is a direct consequence of defining the CISPD using the initial properties. RD and MD present similar levels of energy dissipation as well, even if RD defines a 3% damping ratio for the first and third mode, while MD imposes 3% damping ratio to all the modes of the structure. Finally, the curves of energy dissipated by the TTSPD and CTSPD have an equivalent response for this particular case study.

The subtraction of the energy input and the energy dissipated by the damping model gives the cumulative energy dissipated by the hysteretic rules of the materials. When TISPD and CISPD are used, the energy dissipated through the hysteretic rules present a similar level of energy dissipation and the total energy is less than 80% of the energy dissipated when TTSPD or CTSPD are used. Additionally, when RD and MD are used, the energy dissipated by the materials presents also a similar response, which is only slightly less than the models proportional to the tangent stiffness matrix. The different levels of energy dissipation through the hysteretic rules of the materials mean that the elements with higher demands are in the structure with tangent stiffness proportional damping, where the effective damping ratio will decrease due to the stiffness decay in the structure, which is usually accepted as physically meaningful.

As explained in Section 1, TISPD and RD (using the total initial stiffness) are considered to be inappropriate in nonlinear dynamic analysis. For this specific case, the comparatively high levels of energy dissipation of MD and CISPD may suggest that these models are physically less justifiable than the models proportional to the tangent stiffness matrix.

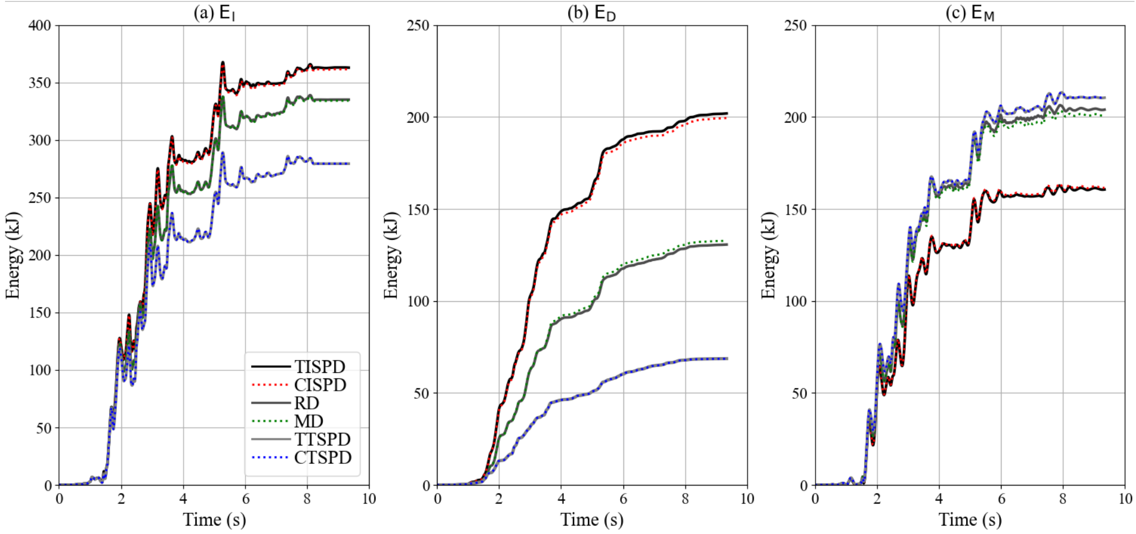

Fig. 2 - (a) Input energy, (b) cumulative energy dissipated by the damping model, and (c) cumulative energy dissipated by the hysteretic rules of the materials.

Figure 1(a-c) shows the damping moments in the rotational DoF of the top left node for the various damping models. As discussed in Section 1, the stiffness proportional term of Rayleigh damping causes spurious damping forces and moments in the massless DoFs when the structure undergoes incursions into the inelastic range. One aspect to note with TISPD is that the spurious damping moments do not disappear even when the structure returns to a response in the elastic range. The latter is explained by the permanent loss of orthogonality in the system due to decay of stiffness in the concrete fibers during the earthquake loading. Oppositely, the TTSPD presents peaks of smaller absolute value during incursions in the inelastic range, and during unloading and reloading in the elastic range the spurious damping moments disappear because the system recovers its orthogonality due to the use of the tangent stiffness to define the damping matrix.

The damping matrix is defined with zeros in the massless DoFs when condensed damping models are used, effectively implying that the spurious damping moments are eliminated: this has been the main argument to justify the use of condensed damping models. Nevertheless, the energy analysis presented in this paper shows that the condensed damping models proportional to the initial properties can cause an overdamped response of the structure, which will imply unconservative analyses, especially in RC structures where there can be important levels of stiffness decay. The TTSPD is the model that has to date better predicted experimental results (Petrini et al. 2008; Chambreuil et al. 2021), but this model still presents important spurious damping moment as can be seen in the figure below. The model that completely eliminates the spurious damping moments and does not present high levels of energy dissipation, preserving a physically consistent interpretation, is the CTSPD herein proposed.

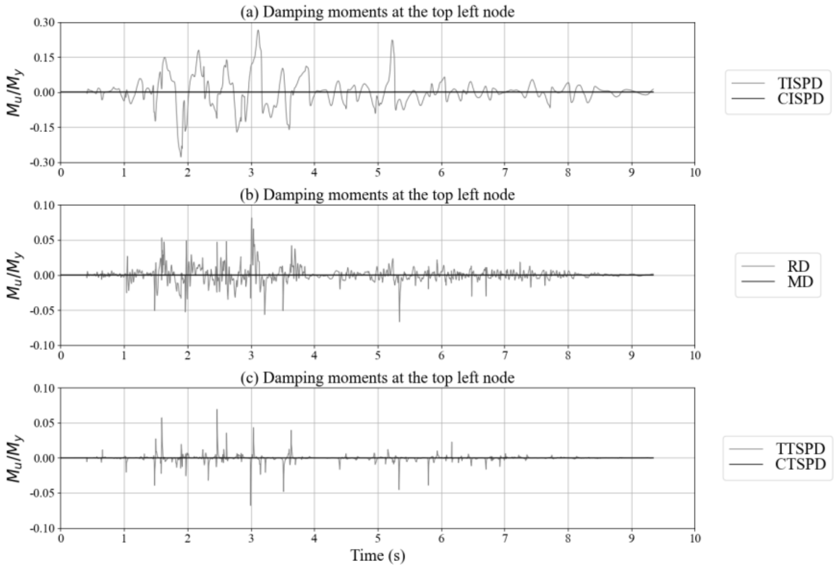

Figure 1 Damping moments at the top left node of the RC frame for the various damping models (note the different vertical scales).

4. Conclusions

This paper investigates the response of a proposed viscous damping model based on a tangent condensed stiffness proportional matrix. The latter is shown to eliminate spurious damping forces and avoids the high levels of damping presented by the condensed damping model defined with the initial properties. This approach also preserves a solid physical meaningfulness related to a reduction of the damping energy when hysteretic material response is activated. Through a case study, it was also seen that the condensed-initial-stiffness-proportional damping and modal damping can have similar levels of energy dissipation than the total initial stiffness proportional damping and Rayleigh damping models. These are generally considered as inappropriate for nonlinear analysis due to spurious damping forces and increments on the effective damping ratio due to the stiffness decay. Such high levels of energy dissipation can affect considerably the total energy absorbed by the nonlinear hysteretic rules of the materials.

5. Acknowledgements

The authors want to express their gratitude to the Fonds Speciaux de Recherche of UCLouvain for funding this research framed in the Grant FSR 2018 and FSR 2021.

6. References

Bernal D (1994) Viscous damping in inelastic structural response. Journal of Structural Engineering 120:1240–1254

Calabrese A, Almeida JP, Pinho R (2010) Numerical issues in distributed inelasticity modeling of RC frame elements for seismic analysis. Journal of Earthquake Engineering 14:38–68. https://doi.org/10.1080/13632461003651869

Carr A (2007) Ruaumoko Theory Manual. University of Canterbury, Christchurch, New Zealand

Chambreuil C, Giry C, Ragueneau F, Léger P (2021) Seismic energy dissipation in reinforced concrete beam: investigating damping formulations. European Journal of Environmental and Civil Engineering 1–27. https://doi.org/10.1080/19648189.2021.2009380

Charney FA (2008) Unintended consequences of modeling damping in structures. Journal of Structural Engineering 134:581–592

Charney F, Lopez-Garcia D, Hardyniec A, Ugalde D (2017) Modeling inherent damping in nonlinear dynamic analysis. 16th World Conference on Earthquake Engineering

Chopra AK (2015) Dynamics of structures theory and applications to earthquake engineering, Fourth edition. Prentice Hall, Boston, USA

Chopra AK, Mckenna F (2016) Modeling viscous damping in nonlinear response history analysis of buildings for earthquake excitation. Earthquake Engineering and Structural Dynamics 45:193–211. https://doi.org/10.1002/eqe.2622

Chrisp D (1980) Damping models for inelastic structures. Master's Thesis, University of Canterbury, Christchurch, New Zealand

Correia A, Almeida JP, Pinho R (2013) Seismic energy dissipation in inelastic frames: understanding state-of-the-practice damping models. Structural Engineering International: Journal of the International Association for Bridge and Structural Engineering (IABSE) 23:148–158. https://doi.org/10.2749/101686613X13439149157001

Erduran E (2012) Evaluation of Rayleigh damping and its influence on engineering demand parameter estimates. Earthquake Engineering and Structural Dynamics 41:1905–1919. https://doi.org/10.1002/eqe.2164

Golesorkhi R, Joseph LM, Klemencic R, et al (2017) Performance-based seismic design for tall buildings : an output of the CTBUH Performance-Based Seismic Design Working Group. CTBUH Headquarters, Chicago, USA

Hall JF (2016) Discussion of 'Modelling viscous damping in nonlinear response history analysis of buildings for earthquake excitation' by Anil K. Chopra and Frank McKenna. Earthquake Engineering and Structural Dynamics 45:2229–2233

Jehel P, Léger P, Ibrahimbegovic A (2014) Initial versus tangent stiffness-based Rayleigh damping in inelastic time history seismic analyses. Earthquake Engineering and Structural Dynamics 43:467–484. https://doi.org/10.1002/eqe.2357

Kanaan A, Powell G (1973) Drain 2D A general purpose computer program for dynamic analysis of inelastic plane structures with user's guide and supplement. University of California, Berkeley, California

Lanzi A, Luco JE (2018) Elastic Velocity Damping Model for Inelastic Structures. Journal of Structural Engineering 144:04018065. https://doi.org/10.1061/(asce)st.1943-541x.0002050

Leger P, Dussault S (1992) Seismic-energy dissipation in MDOF structures. Journal of Structural Engineering 118:1251–1269

Mander JB, Priestley MJN, Park R (1988) Theoretical stress-strain model for confined concrete. Journal of Structural Engineering 114:1804

Medina RA, Krawinkler H (2003) Seismic demands for nondeteriorating frame structures and their dependence on ground motions. Pacific Earthquake Engineering Research Center, Berkeley, California

Menegotto M, Pinto PE (1973) Method of analysis for cyclically loaded R.C. plane frames including changes in geometry and non-elastic behaviour of elements under combined normal force and bending. IABSE reports of the working commissions 13:15–22. https://doi.org/10.5169/seals-13741

Mondkar DP, Powell GH (1975) ANSR-I General purpose program for analysis of nonlinear structural response. University of California, Berkely, California

Petrini L, Maggi C, Priestley N, Calvi G (2008) Experimental verification of viscous damping modeling for inelastic time history analyzes. Journal of Earthquake Engineering 12:125–145. https://doi.org/10.1080/13632460801925822

Powell Graham H (1973) Drain-2D User's guide. University of California, Berkeley, California

Rayleigh L (1877) The theory of sound, Second Edition. Dover Publications, New York, USA

Ryan KL, Polanco J (2008) Problems with Rayleigh Damping in Base-Isolated Buildings. Journal of structural engineering 134:1780–1784. https://doi.org/10.1061/ASCE0733-94452008134:111780

Sharpe RD (1974) The seismic response of inelastic structures. University of Canterbury, Christchurch, New Zealand

Wilson EL, Clough RW (1962) Dynamic response by step by step matrix analysis. In: Symposium on the use of computers in civil engineering. Laboratorio Nacional de Engenharia Civil, Lisbon, Portugal, pp 45.1-45.14

Wilson EL, Penzien J (1972) Evaluation of orthogonal damping matrices. International Journal for Numerical Methods in Engineering 4:5–10